Investigation of N2 plasma GaAs surface passivation efficiency against air exposure: towards an enhanced diode

Hussein Mehdi, François Réveret, Christine Robert-Goumet, Luc Bideux, Bernard Gruzza, Philip Eric Hoggan, Joël Leymarie, Yamina Andre, Evelyne Gil, Théo Levert, et al.

Investigation of N_2 plasma GaAs surface passivation efficiency against air exposure: towards an enhanced diode

H. Mehdi[a,b], F. Réveret[a], C. Robert-Goumet[a], L. Bideux[a], B. Gruzza[a], P. E. Hoggan[a], J. Leymarie[a], Y. Andre[a], E. Gil[a], B. Pelissier[b], T. Levert[b], D. Paget[c], G. Monier[a,*]

[a] *Université Clermont Auvergne, CNRS,Clermont Auvergne INP, Institut Pascal, F-63000 Clermont-Ferrand, France*

[b] *Univ. Grenoble Alpes, CNRS, CEA/LETI-Minatec, Grenoble INP, LTM, 38000 Grenoble, France*

[c] *Physique de la matière condensée, Ecole Polytechnique, CNRS, Université Paris Saclay, 91128 Palaiseau, France*

* Corresponding author

Adress : Institut Pascal, 4 Avenue Blaise Pascal, 63178 AUBIERE Cedex

E-mail address: guillaume.monier@uca.fr

Abstract

GaAs(001) substrates nitrided with N_2 plasma at various temperatures were investigated after being exposed to air for 40 days. They were studied by means of parallel angle-resolved X-ray photoelectron spectroscopy, scanning electron microscopy, micro-photoluminescence and time-resolved photoluminescence (TRPL). Several nitrided GaAs Schottky diodes were manufactured to find the optimal nitridation conditions for high diode quality. An improvement on the ideality factor was achieved for a diode with 1.3 nm-thick GaN layer grown at room temperature and crystallized at 620 °C. The crystallization process was needed to enhance the air-exposed GaAs photoluminescence efficiency by a factor 15. TRPL measurements showed a spectacular increase in the decay time (×4), even for a sample exposed to air for 2 years. A high level of GaAs surface chemical protection was achieved. Indeed, neither the element arsenic As^0 nor Ga and As oxides states were detected at the GaN/GaAs interface for nitridation at high temperature (500 °C), yielding a 3.1 nm-thick GaN layer. However, for nitridation temperatures above 300 °C, pits with an inversed pyramidal shape and square base were formed at the surface, their size increased as nitridation temperature was raised. These pits acted as non-recombination centers which reduced the GaAs photoluminescence yield.

Keywords

Plasma nitridation, Surface passivation, GaN, GaAs Schottky diode, X-ray photoelectron spectroscopy, time-resolved photoluminescence

1. Introduction

GaAs is a material with direct bandgap and a high electron mobility. It is extensively used for electronic and optoelectronic devices, as well as high-frequency radar systems [1–3]. As a substrate, it is a good candidate for monolithic microwave integrated circuits (MMICs) [4,5]. However, GaAs performance suffers from fast surface oxidation. Indeed, both arsenic and gallium are chemically unstable reacting with oxygen when exposed to air,

forming several oxides [6]. Surface oxides or dangling bonds induce many surface states that pin the Fermi level in the middle of the gap and trap the carriers which limit and degrade device performances [7].

To overcome these issues, several groups have developed various passivation techniques [8]. For metal-oxide-semiconductor applications, interfacial passivation layers such as lanthanide oxynitride layers (LaON, NdON, CeON and GdON) [9] were used between the GaAs substrate and the dielectric gate. Si_xN_y layer was widely employed to passivate the sidewalls of LEDs [10], HBTs and photodiode devices [11–13]. Inorganic sulfide treatments (based on $(NH_4)_2S$ and Na_2S) developed by Yablonovitch *et al.* [14] have been used for several decades to passivate GaAs surface through the formation of Ga-S bonds [15]. Other solutions involving $P_2S_5/(NH_4)_2S$ [16], P_2S_5/NH_4OH [17], HCl, HCl:Isopropanol [18] have also been explored. Unfortunately, the treatment of GaAs surface with these solutions has a passivation effect of only a few hours under air exposure before reoxidation [19]. Therefore and also because it is complicated to integrate these wet passivations into an industrial processes, alternative passivations were investigated. They involve growth of a thin interfacial layer with high chemical and thermal stabilities and wide bandgap such as TiN [20], AlN [21,22] and GaN [23]. Surface nitridation of GaAs allowing the growth of a GaN thin layer has been meaningfully studied [24–26]. However, very little previous work has beed reported in the literature studying nitride layer passivation efficiency towards air exposure [27,28].

In this work, we investigate GaAs (001) nitridation by N_2 plasma under various conditions. The aim is to improve the chemical, optical and electrical passivation efficiency after ambient air exposure. To this end, several specific and accurate characterization techniques as parallel angle-resolved X-ray Photoelectron Spectroscopy (pAR-XPS), micro-photoluminescence (µPL) and time-resolved photoluminescence (TRPL), scanning electron microscopy (SEM) and electrical measurements were carried out to analyse the surface morphology, oxidation, and photoluminescence efficiency including the carrier recombination dynamics and the electrical behavior of the nitrided GaAs substrates.

2. Experimental

GaAs (001) substrates with a n-doping level of 4.9×10^{15} cm^{-3} were used. All samples were firstly cleaned following the procedure developed by Tereshchenko *et al.* [18] yielding a (4×1) Ga rich surface reconstruction after annealing at 530 °C in the ultra high vacuum (UHV) chamber. The nitridation process was then carried out using a N_2 plasma commercial electron resonance cyclotron source (SPECS MPS-ECR), operating in atom beam mode at a pressure of 10^{-2} Pa with a sample current density around 10 nA/cm^2, installed in a UHV chamber and described elsewhere [29]. The flux of nitrogen atoms reaches the sample surface through the pressure difference between the plasma source and the UHV chamber. Nitridation was carried out at various temperatures (from room temperature (RT) to 500 °C). It was either followed by annealing at 620 °C or not. The annealing aimed to crystallize the GaN layer formed on the surface. Results for six samples are summarized in Table 1. More details on the growth kinetics of a GaN thin layer on GaAs(001) by N_2 plasma nitridation and its crystallization are given in Refs. [29,30]. The E0 sample is a non-nitrided GaAs substrate. All samples were exposed to air for 40 days after their preparation and before investigation. In view of estimating ageing degradation, the E2’ sample is the E2 sample exposed to air for 2 years.

Table 1 : Nitridation conditions of GaAs (001) samples using ECR source at 10^{-2} Pa annealing at 620 °C. The nitride layer thicknesses are derived from the pAR-XPS measurements.

Samples	Nitridation temperature (°C)	Nitridation time (min)	Annealing at 620 °C	Thickness of GaN (nm)
E0 and E0b	Untreated	-	-	-
E1	RT	180	-	1.3
E2 and E2’	RT	180	x	
E3	400	60	-	1.5
E4	400	60	x	
E5	500	60	-	3.1
E6	500	60	x	

Parallel Angle-Resolved X-ray photoelectron spectroscopy (pARXPS) measurements were carried out using a ThermoFisher Scientific Theta 300 tool with a monochromatised Al-Kα source (beam spot size of 400 µm), a pass energy of 100 eV and an electron gun for surface charge compensation. The pARXPS spectra were recorded simultaneously at seven different take-off angles (with respect to the sample normal) between 23.75° to 61.25° with no sample tilt. This method determines a concentration surface profile of the nitride layer grown on GaAs.

Micro-photoluminescence (µPL) measurements were performed at low temperature (5 K; using a liquid helium circulation closed cycle cryostat) with a continuous 514 nm wave line of argon ion laser as excitation source with a power density of 14 W/cm² and a spot size around 30 µm-diameter. The emitting signal was focused on the slit of a 100 cm focal monochromator using a grating with 1200 g/mm and coupled to CCD camera. Ten measurements were carried out at different sample positions (spaced by 400 µm on a 4 mm line) to obtain a good accuracy.

Time-resolved photoluminescence (TRPL) was performed at 5 K using the same cryostat. The excitation source was a Ti:Sa pulsed laser emitting at 770 nm with a pulse duration of 150 fs and a repetition rate of 76 MHz. The photoluminescence signal was collected in a 32 cm focal monochromator using a grating with 300 g/mm coupled with a streak camera. For all TRPL measurements, the given power is the average power per surface unit.

Scanning electron microscopy was carried out using a ZEISS Ultra-55VP.

Four Schottky diodes were made using E0 and three nitrided samples (E1, E2 and E5). Ohmic contacts were deposited on the back side of the GaAs substrate by sequential evaporations of Au(1000nm)/Ge(35nm)/Au(10nm) through a hard mask of molybdenum at 10^{-4} Pa. An annealing process at a temperature between 200 and 350 °C in H_2 environment was applied to allow the diffusion of Ge species creating a thin n^+ layer necessary for good quality contact. Then, Au dots with a diameter of 600 µm and thickness of 100 nm were grown on the front side of the samples (Schottky contact) exposed 40 days in ambient air. These dots were manufactured under UHV at room temperature using a calibrated Knudsen cell Au flow through a hard mask of molybdenum having 4 holes. A sample E0b is used as a reference to study the effect of oxidation due to air exposure on the electrical performances of GaAs Schottky diodes. The sample E0b undergoes the same cleaning and heating processes than E0 but Au dots were deposited in situ (without air exposure). Current-voltage measurements were performed in dark at room temperature using Keithley 2636 source meter from -2 V to 2 V on the four Au dots. For each sample, similar electrical characteristics were obtained on, at least, three dots.

3. Results and discussion

3.1 Chemical passivation

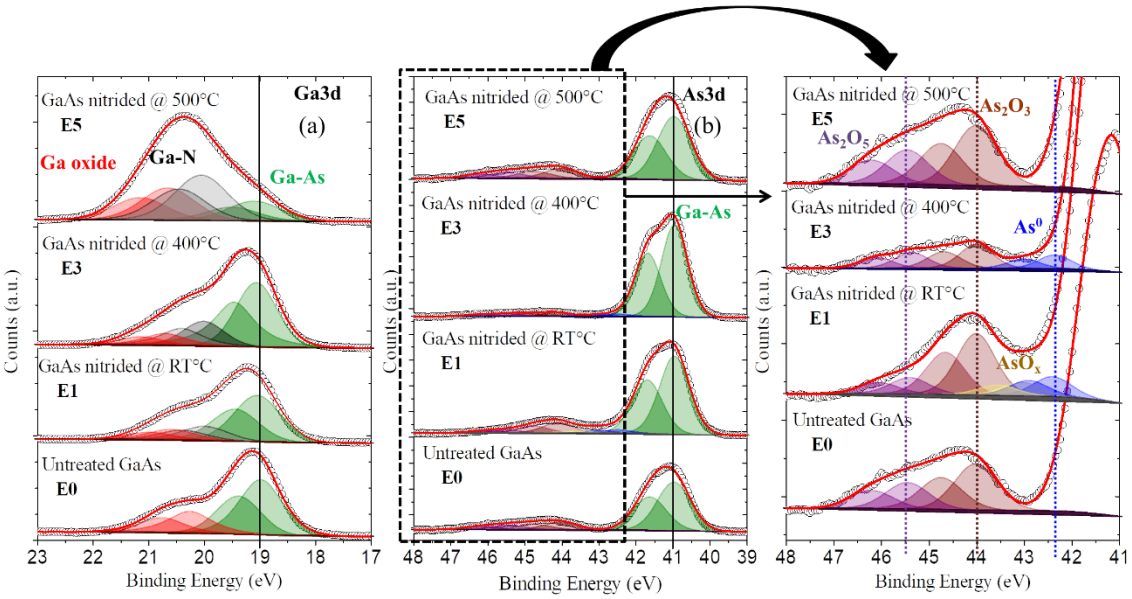

Figure 1 : (a) Ga3d and (b) As3d spectra from pAR-XPS analysis for untreated sample E0 (not nitrided) and E1, E3 and E5 nitrided GaAs(001) samples at different temperature after 40 days of air exposure for a take-off angle of 23.75°

Figure 1(a) and 1(b) show the Ga3d and As3d peaks measured by pAR-XPS at a take-off angle of 23.75°, for untreated GaAs (E0 sample) and samples nitrided at RT (E1), 400 °C (E3) and 500 °C (E5) after 40 days of air exposure. The decompositions of As3d and Ga3d peaks are based on chemical shifts already described in previous results obtained before air exposure [29]. All the spectra are calibrated in energy with respect to the chosen reference As-Ga component in As3d peak located at 41.0 eV. Four other components are identified in the As3d peak: free arsenic atoms As^0 at 42.4 eV, AsO_x at 43.1 eV (this small contribution is ascribed to incomplete As oxidation), As_2O_3 at 44.1 eV and As_2O_5 at 45.5 eV [31–33]. Only the two last arsenic oxidation states are identified for E0 corresponding to the native oxide. The free arsenic As^0 component is detected only for samples nitrided at a temperature < 500 °C, as shown in the As3d spectra for E1 and E3 samples.

Three components are detected in the Ga3d peak (Fig. 1(a)): the main component at 19.0 eV corresponds to Ga-As bonds related to GaAs substrate, the second component at 20 eV is ascribed to Ga-N bonds (detected only for nitrided samples), and the third one around 20.3-20.6 eV relates to gallium oxides (named Ga oxide in Fig. 1(a)). This third component stems from gallium oxide (Ga_2O_3) [6,34] corresponding to the native oxide for E0, and Ga-O bonds in the nitride layer due to a few oxygen atoms incorporated during the nitriding process as already observed previously [29] and the air exposure. Note that the same contributions are observed in the Ga3d and As3d peaks for nitridation carried out at temperatures up to 400 °C.

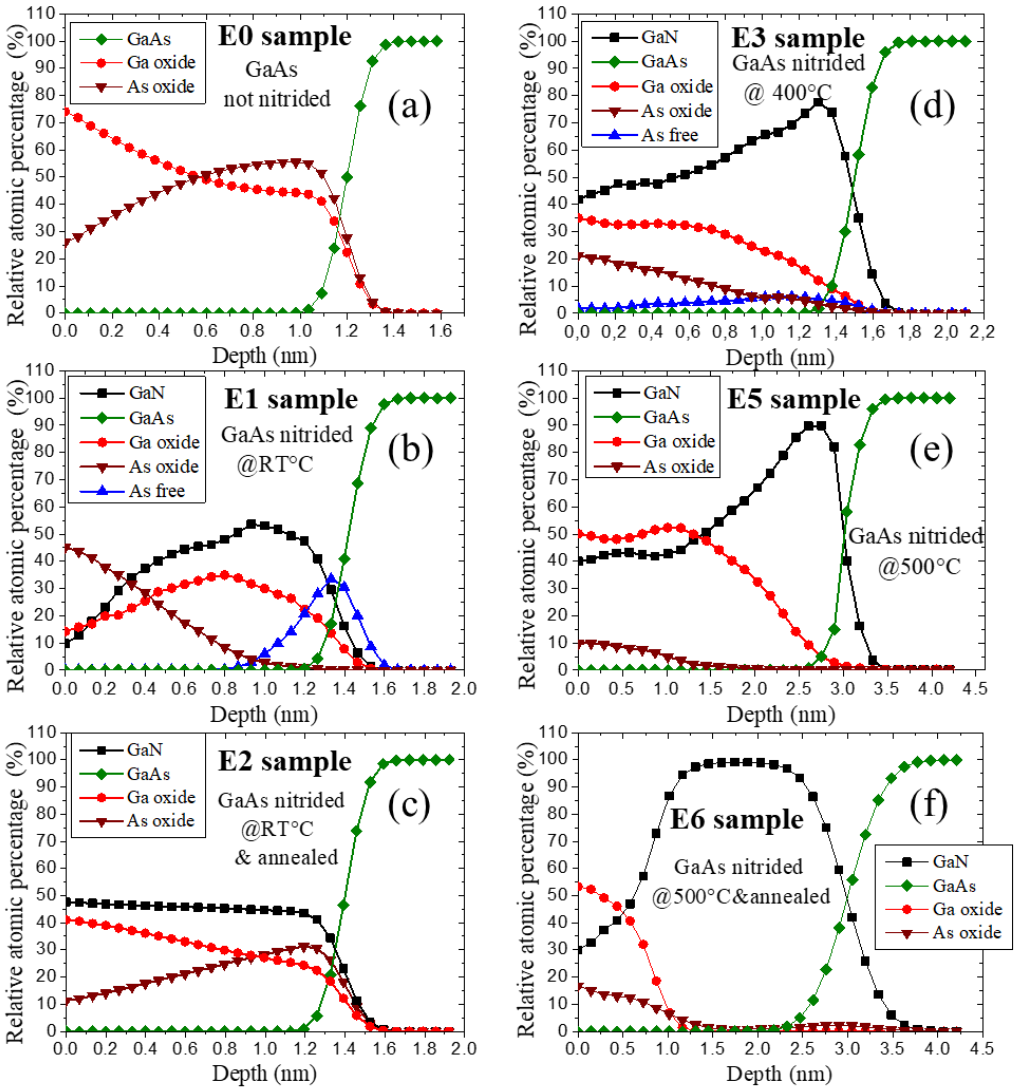

Figure 2 : Chemical profile reconstruction obtained by pAR-XPS for (a) untreated GaAs (E0 sample) and nitrided GaAs(001) (b) at RT without and (c) with annealing at 620 °C, (d) at 400 °C and (e) at 500 °C without and (f) with annealing at 620 °C.

Figure 2 shows the chemical profile reconstruction obtained from pAR-XPS data using Avantage software developed by ThermoFisher Scientific where the entropy maximization method coupled with least-squares fitting is used [35]. In this figure, the relative atomic percentage (at.%) of GaAs, GaN, Ga oxides, As oxides (including AsO_x, As_2O_3, As_2O_5) and free arsenic atoms As^0 are plotted as a function of depth.

Fig 2a shows the reference case of the untreated GaAs surface (E0 sample). As previously observed [36] this figure reveals the presence of a 1.2 nm-thick native oxide. The gallium and arsenic oxide quantities are inhomogeneously distributed in the oxide layer. Gallium oxide represents 75 at.% at the top surface, decreasing to 50 at.% at 0.6 nm-depth. Beyond this depth, the amount of gallium and arsenic oxides are similar up to the oxide/GaAs interface.

As shown from Figs. 2(b) and 2(d), nitriding the GaAs at a temperature lower than 500 °C induces accumulation of free As^0 at the GaN/GaAs interface. In the case of nitridation at RT, an As^0 quantity of 30 at.% is obtained whereas when heating is applied, As^0 concentration is lower at around 6 at.% for 400 °C. This phenomenon is caused by the outward diffusion of As^0 in the GaN layer created, due to heating and its desorption at a temperature above 320 °C [37]. This behavior is consistent with the composition profiles obtained in Ref. [29] for nitrided samples that have not been exposed to air. However, a part of the remaining

free As^0 created during nitridation is oxidized during air exposure, which leads to the presence of As oxides at the surface. Note that no arsenic oxide was detected before air exposure. This oxide amount which is around 50 at.% at the surface for nitridation at RT, is reduced when the nitridation temperature is increased, to only 10 at.% for nitridation at 500 °C (Fig. 2(e)). Nevertheless, the As oxides remain localized in the first nm of the nitride layer. Although the gallium oxides are distributed more evenly in the nitride layer due to their unintentional incorporation during the nitridation process, their quantity, estimated between 25 and 50 at.% at the surface, decreases with the depth to almost 0 at.% at the GaN/GaAs interface. Note that their average quantity in the nitride layer estimated at 10 at.% before air exposure with the modelling developed in Ref. [29] increased to around 35 at.% after air exposure. The GaN concentration follows the opposite trend as it increases to reach up to 90 at.% at the GaN/GaAs interface for the nitridation at 500 °C. Hence, we conclude that only part of the outermost nitride layer is oxidized upon air exposure.

The effect of annealing the nitride layer at 620 °C is shown in Figs. 2(c) and 2(f). The main change observed for the sample nitrided at RT (E2) is the desorption of the free As^0 atoms during the heating. The As and Ga oxides remain present in the nitride layer. Conversely, annealing the sample nitrided at 500 °C considerably rarifies the Ga oxides, which are localized in the first nanometer of the nitride layer. Thus no oxide is present at the GaN/GaAs interface revealing the best chemical passivation treatment with these experimental conditions.

3.2 Electrical characterization

Electrical measurements I-V at room temperature in dark for E0, E1, E2 and E5 samples are shown in Fig. 3. Using the forward bias part of these spectra, the ideality factor (n), the saturation current (I_0), the barrier height (ϕ_{b0}) and the series resistance (R_s) are extracted using the method explained in Refs. [38,39]. They are listed in Table 2.

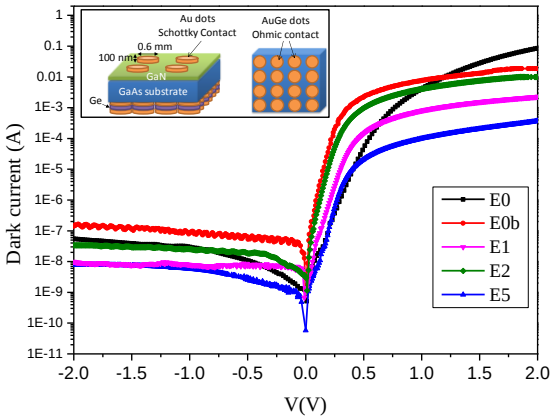

Figure 3 : I-V characteristic of Schottky diodes manufactured with E0, E0b, E1, E2 and E5 samples

Table 2 Extracted electrical parameters from I-V characteristics from Fig. 3.

Samples	n	I_s (A)	Φ_{b0}(eV)	Rs (Ω)
E0	1.80	1.4×10^{-9}	0.72	33
E0b	1.23	1.5×10^{-10}	0.80	90
E1	1.38	4.4×10^{-9}	0.69	692
E2	1.24	2.2×10^{-8}	0.65	149
E5	1.30	3.1×10^{-10}	0.76	451

Considering the non-nitrided sample, E0 exhibits a high ideality factor of 1.80 due to the 1.1 nm-thick native oxide layer containing Ga_2O_3, As_2O_3 and As_2O_5 as detected by pAR-XPS. Thus, the electrical characteristic of this diode follows more a metal-insulator-semiconductor (MIS) configuration than an ideal Schottky diode behavior.

Considering nitrided samples, the ideality factors of E1, E2 and E5 are 1.38, 1.24 and 1.30, respectively. These samples also follow non-ideal Schottky behavior caused by the nitrided GaAs surface oxidation occurring

during the 40 days of air exposure before the gold deposition. However, sample E2 has the same ideality factor (1.24) than the reference sample E0b on which the Schottky metal deposit is fabricated under UHV (1.23). This demonstrates the efficiency of this nitridation process.

Moreover, E5 has the highest zero-bias barrier height at 0.76 eV close to the value of the sample E0b (0.80eV) which is consistent with the value obtained by Leroy *et al.*[40] on 260nm-Au/n-GaAs diodes showing an average barrier height of 0.819 eV and close to 0.83, 0.89, 0.86 and 0.816 eV values reported in the literature [41–44]. The barrier height of E1 and E2 samples were found to be lower at 0.69 and 0.65 eV, respectively. This can be explained by the presence of As atoms in the GaN/GaAs structure (up to 35% at GaN/GaAs interface) as can be seen in the depth profile compositions of Fig 2 (b). Indeed, this presence leads (i) to a shift of the fermi level toward conduction band minimum (CBM) and (ii) to increase the filling of As_{Ga} antisites relative to the number of Ga_{As} antisites, which both induce a decrease of ϕ_{b0} [45]. Conversely, the sample E5 nitrided at high temperature (500 °C) for which the As atoms are totally desorbed (Fig 2(e)), shows a higher barrier height of 0.76 eV. The high series resistance for E1, E2 and E5 is the consequence of the undoped GaN thin layer growth containing several oxides states as shown in §3.1. Thus, E5 sample shows the best electrical performance which is consistent with its highest chemical passivation (reduced amount of arsenic and gallium oxides at the GaN/GaAs interface). Note that the measured electrical characteristic on this sample exhibits enhanced values [46], including a very low saturation current of 3.1×10^{-10} A.

3.3 Optical characterization

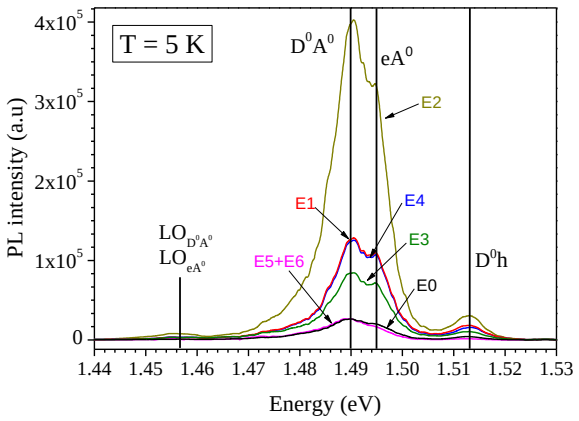

Figure 4 : µPL spectra of untreated (E0) and nitrided GaAs(001) substrates (E1-E6) at 5K with an excitation power density of 14 W/cm^2.

µPL spectra for samples E0-E6 are shown in Fig. 4. Same transitions are detected for all these samples; two dominant peaks are observed at 1.490 and 1.495 eV corresponding to both the transitions between neutral donor and neutral acceptor (D^0-A^0) and that for band conduction and neutral acceptor (e-A^0) respectively [47–50]. A low emission observed around 1.450 eV is linked to the two longitudinal optical phonon replicas (order 1) of (D^0-A^0) and (e-A^0) transitions [50]. The emission centred at 1.513 eV mainly corresponds to neutral donors to valence band (D^0-h), ionized donors to exciton transitions can also be detected close to this energy [49].

All nitrided samples show higher µPL intensity compared to the untreated one (E0 sample) except those nitrided at 500 °C (E5 and E6 samples) as shown in Fig. 4. Photoluminescence intensity of the main peak (D^0-A^0) for E1 and E4 samples are increased by a factor of 5 compared to the untreated E0 sample. This factor is decreased to 3 for E3 sample and increased to 15 for E2 sample [17,27,51]. Clearly, increasing the nitridation temperature from RT to 500 °C has an impact; reducing improvement in the GaAs photoluminescence, while the optimal surface chemical passivation is obtained at high nitridation temperature (500 °C) with annealing at 620 °C as shown in §3.1.

To understand this behavior, SEM images of E1, E2, E4 and E5 surfaces were performed (Fig. 5). Samples nitrided at a temperature higher than 400 °C (E3, E4, E5 and E6 samples) show pits at their surfaces having an inversed pyramidal shape with a square base as shown in Figs. 5(c) and 5(d). The increase of the nitridation temperature has an impact on the size of the pits. Indeed, pits observed on E5 and E6 surfaces nitrided at 500 °C

have a size between 150 and 300 nm larger than those formed on E3 and E4 samples nitrided at 400 °C having a size between 40 and 80 nm. Note that the annealing process does not change either the size or the number of these pits (not shown here). During the nitridation process, the exchange between As and N atoms induces the decomposition of Ga-As bonds as explained in previous work [29]. Moreover, a microscopy investigation carriedout on a similar sample [30] shows threading dislocations (TDs) generated at GaN/GaAs interface. These TDs relieve the tensile strain due to the high lattice mis-match between GaAs and GaN (~20%). The GaAs {101} facets have lower surface formation energy meaning that they are more stable than GaAs {111} facets. Hence, we believe that increasing the nitridation temperature accelerates the decomposition of GaAs {111} facets, explaining that at low temperature (below 350 °C), these pits are not observed and giving larger pits when temperature increases. Similar pits have been observed by Tricker *et al*. [52], highlighting their formation by diffusion and desorption of As atoms under As_2 form. Thus it can be deduced that these pits may behave as non-radiative recombination centers which, therefore, limit the photoluminescence.

Crystallization of the nitride layer by annealing at 620 °C induces an increase of PL intensity by a factor of 3.5 and 1.5 for nitridation at RT and 400 °C, respectively. The influence of crystallization vanishes when the nitridation is performed at 500 °C as the non-radiative effect of created pits becomes preponderant. Thus, increasing the nitridation temperature induces the formation of pits which reduces the benefits of surface passivation. The optimum process, from an optical point of view, is therefore a nitridation at room temperature followed by crystallization of the GaN layer by annealing at 620 °C.

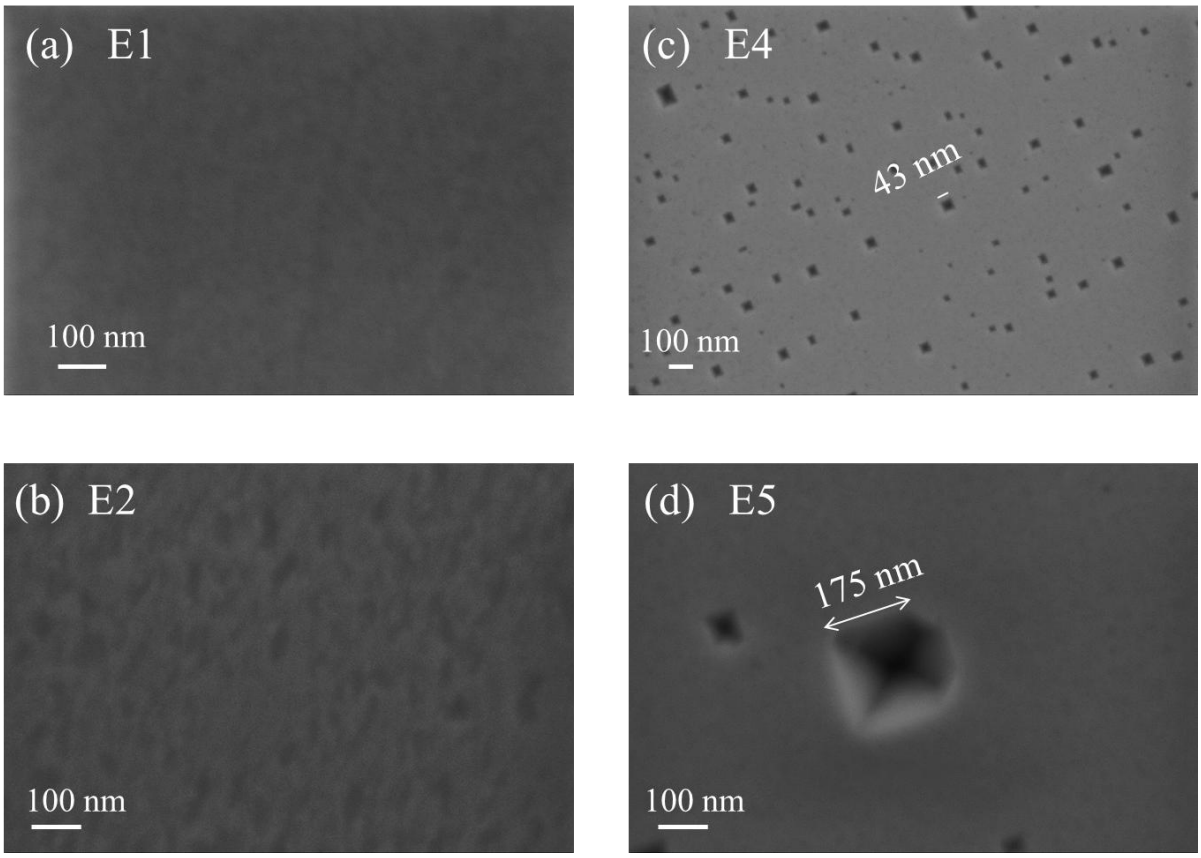

Figure 5 : SEM image of (a)E1, (b)E2, (c)E4 and (d)E5 nitrided sample surface.

To further study the optical advantages of nitriding GaAs, we carried out TRPL measurements. In Fig. 4, the measured µPL signal under continuous wave excitation exhibits a maximum at 1.49 eV while the emission at 1.513 eV is weaker. Under pulse excitation where the power density is much higher, the response of the sample appears different. As observed in Fig. 6 the emission at 1.513 eV dominates until 400 ps, then it gradually

disappears while the contribution at 1.49 eV persists even after 1800 ps. Thus, this emission was chosen to monitor the GaAs nitridation effect on the TRPL.

The photoluminescence decay times measured on samples E0, E2, E2' and E4 at 185 W/cm² and at 1.513 eV are shown in Fig. 7. The following equation is used to estimate the decay time of the PL intensity (I_{PL}):

$$I_{PL} = y_0 + A_1 \exp(-t/\tau_1) + A_2 \exp(-t/\tau_2) \qquad \text{(Eq.1)}$$

Where A_i and τ_i are respectively the weight and the decay time of each contribution and y_0 is a constant to take into account the long decay time induced by the 1.49 eV transition.

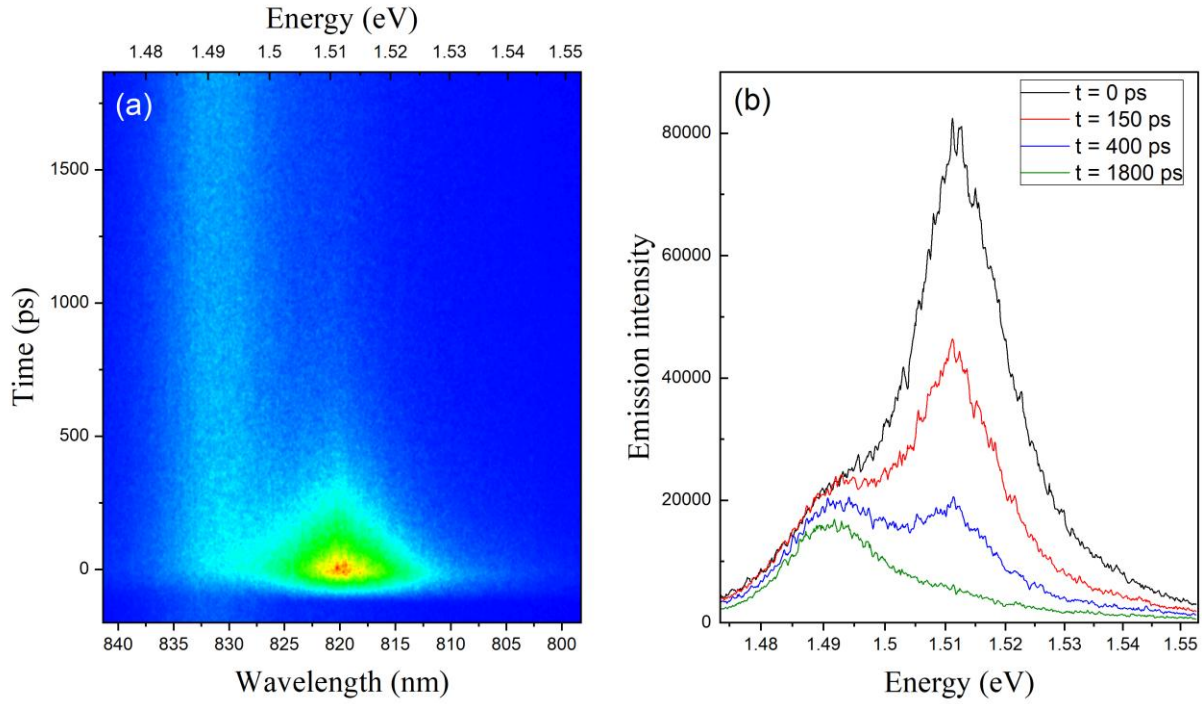

Figure 6 : (a) Time-resolved photoluminescence picture recorded on sample E2 at 185 W/cm². (b) PL spectra of emission intensity versus energy taken from (a) at 0, 150, 400 and 1800 ps.

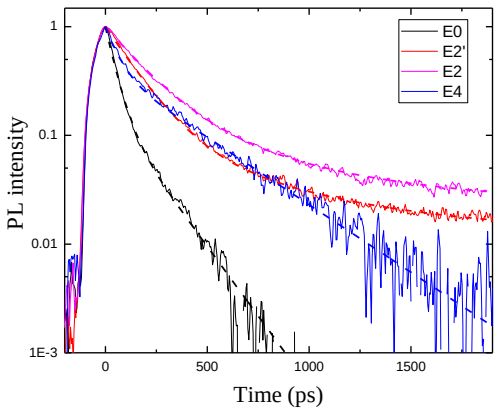

Figure 7 : Comparison of decay times measured on samples E0, E2, E2' and E4 at 185 W/cm² and at 1.513 eV. Fits are done using the bi-exponential equation (Eq.1) (dashed lines).

The parameters extracted from the fit using equation (Eq.1) and shown in Fig. 7 are reported in Table 3. All spectra are dominated by the shorter decay time. Indeed, the ratios of A_1 over A_2 are equal to 10.3, 5.7, 4.9 and 1.5 for samples E2', E2, E0 and E4, respectively.

Table 3 : y_0, A_i and τ_i extracted from the fit of sample E0, E2, E2' and E4 at 185 W/cm².

	E0	E2	E2'	E4
y_0 (%)	0	2.4	1.3	0
τ_1 (ps)	45	180	145	60
A_1 (%)	83	83	90	60
τ_2 (ps)	130	600	600	350
A_2 (%)	17	14.6	8.7	40

The decay times recorded for sample E2 at 1.513 eV for power densities in the range of 37 to 370 W/cm² are reported in Fig. 8(a). The power dependent decay time (τ_1) for samples E0, E2, E2' and E4 are compared in Fig. 8(b). For all samples, an increase of the decay time with optical pumping is clearly observed. However, the increase is moderate for samples E0 and E4 and strong for both samples E2. When the optical pumping intensity is increased the non-radiative channel is saturated which induces a rise of the measured decay time. If we compare the decay time of the nitrided samples with the reference sample at 185 W/cm², we obtain a factor of 1.33, 3.2 and 4 for E4, E2' and E2, respectively. As observed on the PL intensity in Fig. 4, sample E2 exhibits the most improvement.

Our results are in good agreement with the work of Zou *et al.* [28], who also observe an improvement in both PL intensity and decay time. However, here we demonstrate that our nitridation process offers a long lifetime enhancement of the optical properties, remaining stable for 2 years of air exposure which is better than results reported for other nitridation passivations [27,53].

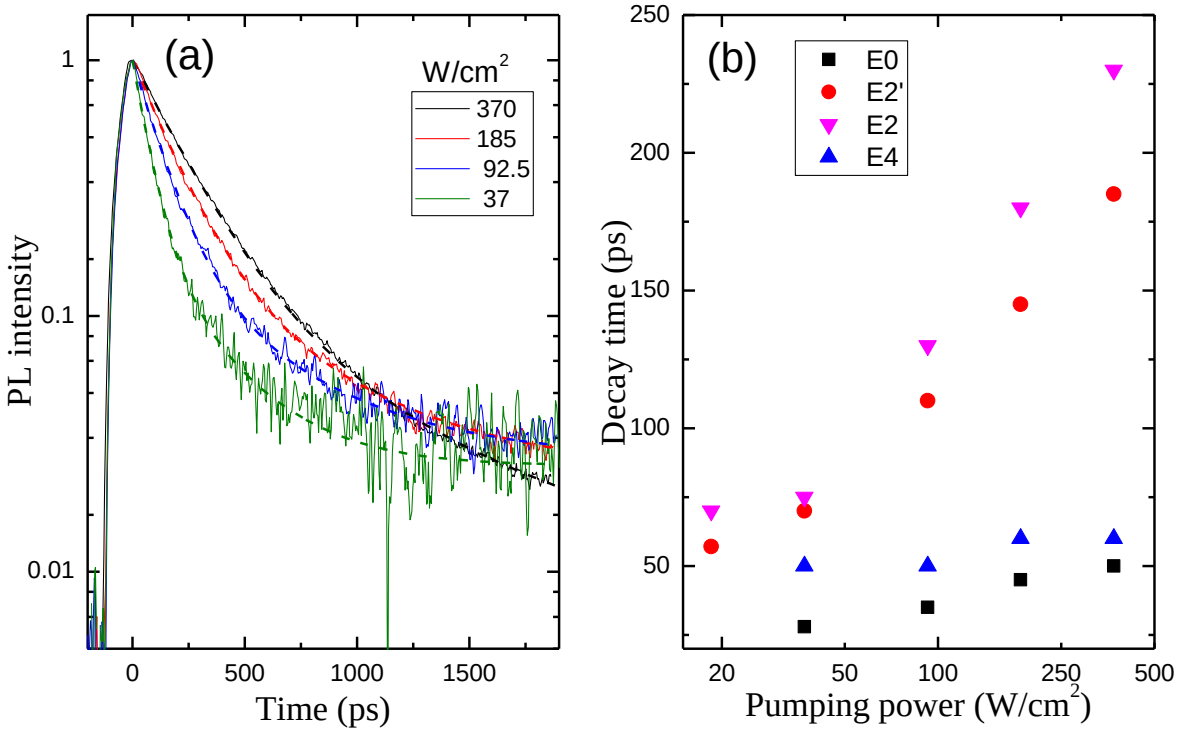

Figure 8 : (a) Decay time measurements from 37 to 370 W/cm² for sample E2 at 1.513 eV (Fits are done using the bi-exponential equation (Eq.1) (dashed lines)). (b) Evolution of τ_1 for samples E0, E2, E2' and E4 from 18.5 to 370 W/cm² at 1.513 eV.

Conclusion

It was proven, in this work, that the nitridation temperature, GaN thickness and its crystallization play a crucial role in GaAs (001) surface passivation. Indeed, the chemical protection of the GaAs surface against oxidation depends on nitridation conditions. This is also the case of enhanced PL emission and extended carrier life time of the GaAs or better electrical characteristics.

Effective chemical passivation of GaAs surface was established by nitridation at high temperature (500 °C), yielding a 3 nm-thick GaN layer. Furthermore, Ga and As oxides were undetected at the GaN/GaAs interface. Yet, many pits were formed at the nitrided GaAs surface for such a high temperature. These pits trap the charge carriers showing a very weak photoluminescence. Therefore, the optimal process for high GaAs photoluminescence and carrier lifetime consists in a nitridation at low temperature followed by an 620°C annealing. This passivation process offered a enhancement by a factor 15 of the PL intensity and a very high stability over lengthy air exposure times, even after 2 years. We demonstrated a major improvement of the GaAs based Schottky diode parameters after the same nitridation process compared to those with an untreated GaAs surface. However, the optimal electrical characteristics (Table 2) were obtained for the nitridation process carried out at 500 °C, exhibiting a similar ideality factor than for a GaAs schottky diode fabricated *in situ* under UHV.

Thus, nitridation parameters must be tuned depending on the targeted GaAs-based device. We can state that the nitridation processes described in our study could be installed in industrial process lines, opening a new versatile way of improving the performances of GaAs devices. In addition, we have already demonstrated the benefits of nitridation process with N_2 plasma to homogeneously passivate nano-objects such as nanowires over their whole surface [54,55].

Acknowledgement

This work has been financially supported by the CPER MMASYF of Region Auvergne-Rhone Alpes that we acknowledge gratefully. It was also funded by the program “Investissements d’avenir” of the French ANR agency, the French governement IDEX-SITE initiative 16-µIDEX-0001 (CAP20-25), the European Commission (Auvergne FEDER Funds), and the Region Auvergne in the framework of the LabEx IMobS3 (ANR-10-LABX-16-01) and CPER.

References

[1] S. Mokkapati, C. Jagadish, III-V compound SC for optoelectronic devices, Mater. Today. 12 (2009) 22–32. doi:10.1016/S1369-7021(09)70110-5.

[2] C. S. Harder, B. J. Van Zeghbroeck, M. P. Kesler, H. P. Meier, P. Vettiger, D. J. Webb, P. Wolf, High-speed GaAs/AlGaAs optoelectronic devices for computer applications, IBM J. Res. Dev. 34 (1990) 568–584. doi:10.1147/rd.344.0568.

[3] J. Yoon, S. Jo, I. Su Chun, I. Jung, H. Sik Kim, M. Meitl, E. Menard, X. Li, J. J. Coleman, U. Paik, J. A. Rogers, GaAs photovoltaics and optoelectronics using releasable multilayer epitaxial assemblies, Nature. 465 (2010) 329–333. doi:10.1038/nature09054.

[4] N. Deo, Microwave and millimeter wave solid state power amplifiers for future space-based communications and radars, 2018 IEEE Aerosp. Conf. (2018) 1–7. doi:10.1109/AERO.2018.8396707.

[5] D. Platt, L. Pettersson, D. Jakonis, M. Salter, J. Haglund, Integrated 79GHz UWB automotive radar front-end based on Hi-Mission MCM-D silicon platform, Int. J. Microw. Wirel. Technol. 2 (2010) 325–332. doi:10.1017/S1759078710000462.

[6] L. Feng, L. -dong Zhang, H. Liu, X. Gao, Z. Miao, H. -chang Cheng, L. Wang, S. Niu, Characterization study of native oxides on GaAs(100) surface by XPS, Proc. SPIE 8912, Int. Symp. Photoelectron. Detect. Imaging 2013 Low-Light-Level Technol. Appl. 89120N. (2013) 16 August.

doi:10.1117/12.2033679.

[7] R. J. Krantz, D. C. Mayer, W. L. Bloss, The influence of Fermi-level pinning at the GaAs substrate on HEMT threshold voltage, Solid State Electron. 33 (1990) 1189–1195. doi:10.1016/0038-1101(90)90098-Y.

[8] H. Hasegawa, M. Akazawa, A. Domanowska, B. Adamowicz, Surface passivation of III-V semiconductors for future CMOS devices-Past research, present status and key issues for future, Appl. Surf. Sci. 256 (2010) 5698–5707. doi:10.1016/j.apsusc.2010.03.091.

[9] L. N. Liu, W. M. Tang, X. D.Huang, J. P. Xu, P. T. Lai, Surface Passivation Using Lanthanide Oxynitrides for GaAs Metal-Oxide-Semiconductor Applications, IEEE Trans. Electron Devices. 66 (2019) 3080–3085. doi:10.1109/TED.2019.2914364.

[10] M. Aziz, C. Xie, V. Pusino, A. Khalid, M. Steer, I. G.Thayne, D. R.S. Cumming, Multispectral mid-infrared light emitting diodes on a GaAs substrate, Appl. Phys. Lett. 111 (2017) 102102. doi:10.1063/1.4986396.

[11] Y.S. Lin, B.Y. Chen, Effects of surface passivation and temperature on AlGaAs/InGaAs high-electron mobility transistor, Microelectron. Eng. 214 (2019) 100–103. doi:10.1016/j.mee.2019.04.028.

[12] A. Jaouad, V. Aimez, Passivation of air-exposed AlGaAs using low frequency plasma-enhanced chemical vapor deposition of silicon nitride, Appl. Phys. Lett. 89 (2006) 092125. doi:10.1063/1.2345030.

[13] H.J. Song, C.H. Roh, J.H. Lee, H.G. Choi, D.H. Kim, J.H. Park, C.K. Hahn, Comparative analysis of dark current between SiNx and polyimide surface passivation of an avalanche photodiode based on GaAs, Semicond. Sci. Technol. 24 (2009) 055012. doi:10.1088/0268-1242/24/5/055012.

[14] E. Yablonovitch, C. J. Sandroff, R. Bhat, T. Gmitter, Nearly ideal electronic properties of sulfide coated GaAs surfaces, Appl. Phys. Lett. 51 (1987) 439. doi:10.1063/1.98415.

[15] D. Paget, A.O. Gusev, V.L. Berkovits, Sulfide-passivated GaAs (001). II . Electronic properties, Phys. Rev. B. 53 (1996) 4615–4622.

[16] Y. Wang, Y. Daraci, P.H. Holloway, Surface passivation of GaAs with P2S5-containing solutions, J. Appl. Phys. 71 (1992) 2746. doi:10.1063/1.351048.

[17] H.H. Lee, R.J. Racicot, S.H. Lee, Surface passivation of GaAs, Appl. Phys. Lett. 54 (1989) 724–726. doi:10.1063/1.100873.

[18] O.E. Tereshchenko, S.I. Chikichev, A.S. Terekhov, Atomic structure and electronic properties of HCl-isopropanol treated and vacuum annealed GaAs(100) surface, J. Vaccum Sci. Technol. A. 17 (1999) 2655. doi:10.1016/S0169-4332(98)00634-5.

[19] M. Rebaud, M. -C. Roure, V. Loup, P. Rodriguez, E. Martinez, P. Besson, Chemical Treatments for Native Oxides Removal of GaAs Wafers, ECS Trans. 69 (2015) 243–250. doi:10.1149/06908.0243ecst.

[20] M. Bosund, A. Aierken, J. Tiilikainen, T. Hakkarainen, H. Lipsanen, Passivation of GaAs surface by atomic-layer-deposited titanium nitride, Appl. Surf. Sci. 254 (2008) 5385–5389. doi:10.1016/j.apsusc.2008.02.070.

[21] M. Bosund, P. Mattila, A. Aierken, T. Hakkarainen, H. Koskenvaara, M. Sopanen, V. M. Airaksinen, H. Lipsanen, GaAs surface passivation by plasma-enhanced atomic-layer-deposited aluminum nitride, Appl. Surf. Sci. 256 (2010) 7434–7437. doi:10.1016/j.apsusc.2010.05.085.

[22] T. Aoki, N. Fukuhara, T. Osada, H. Sazawa, M. Hata, T. Inoue, Nitride passivation reduces interfacial traps in atomic-layer-deposited Al2O3/GaAs (001) metal-oxide-semiconductor capacitors using

atmospheric metal-organic chemical vapor deposition, Appl. Phys. Lett. 105 (2014) 033513. doi:10.1063/1.4891431.

[23] S. Anantathanasarn, S. Ootomo, T. Hashizume, H. Hasegawa, Surface passivation of GaAs by ultra-thin cubic GaN layer Surface passivation of GaAs by ultra-thin cubic GaN layer, Appl. Surf. Sci. 159–160 (2000) 456–461. doi:10.1016/S0169-4332(00)00077-5.

[24] C. Huh, S. Park, S. Ahn, J.Y. Han, K.J. Cho, J.M. Seo, Synchrotron radiation photoemission spectroscopy studies of the thermal nitridation of GaAs (100) with ammonia, J. Vac. Sci. Technol. B. 16 (1998) 192–196. doi:10.1116/1.589776.

[25] K. Uwai, Y. Yamauchi, N. Kobayashi, In situ observation of nitridation of GaAs (001) surfaces by infrared reflectance spectroscopy, Appl. Surf. Sci. 101 (1996) 412–416. http://www.sciencedirect.com/science/article/pii/0169433296003108 (accessed April 4, 2014).

[26] F. Gao, S.J. Lee, D.Z. Chi, S. Balakumar, D.L. Kwong, GaAs metal-oxide-semiconductor device with HfO2/TaN gate stack and thermal nitridation surface passivation, Appl. Phys. Lett. 90 (2007) 111–114. doi:10.1063/1.2749840.

[27] M. Losurdo, P. Capezzuto, G. Bruno, G. Perna, V. Capozzi, N2–H2 remote plasma nitridation for GaAs surface passivation, Appl. Phys. Lett. 81 (2002) 16–18. doi:10.1063/1.1490414.

[28] X. Zou, C. Li, X. Su, Y. Liu, D. Finkelstein-Shapiro, W. Zhang, A. Yartsev, Carrier Recombination Processes in GaAs Wafers Passivated by Wet Nitridation, ACS Appl. Mater. Interfaces. 12 (2020) 28360–28367. doi:10.1021/acsami.0c04892.

[29] H. Mehdi, G. Monier, P.E. Hoggan, L. Bideux, C. Robert-Goumet, V.G. Dubrovskii, Combined angle-resolved X-ray photoelectron spectroscopy, density functional theory and kinetic study of nitridation of gallium arsenide, Appl. Surf. Sci. 427 (2018) 662–669. doi:10.1016/j.apsusc.2017.08.002.

[30] H. Mehdi, F. Réveret, C. Bougerol, C. Robert-Goumet, P.E. Hoggan, L. Bideux, B. Gruzza, J. Leymarie, G. Monier, Study of GaN layer crystallization on GaAs(100) using electron cyclotron resonance or glow discharge N2 plasma sources for the nitriding process, Appl. Surf. Sci. 495 (2019) 143586. doi:10.1016/j.apsusc.2019.143586.

[31] Y. Mizokawa, H. Iwasaki, R. Nishitani, N. Shogo, ESCA studies of Ga, As, GaAs, Ga2O3, As2O3 and As2O5, J. Electron Spectros. Relat. Phenomena. 14 (1978) 129–141.

[32] M. A. Hoffbauer, J. B. Cross, V. M. Bermudez, Growth of oxide layers on gallium arsenide with a High kinetic-energy atomic oxygen Beam, Appl. Phys. Lett. 57 (1990) 2193–2195. doi:Doi 10.1063/1.103933.

[33] Z. H. Lu, B. Bryskiewicz, J. McCaffrey, Z. Wasilewski, M. J. Garham, Ultraviolet-ozone oxidation of GaAs(100) and InP(100), J. Vac. Sci. Technol. B Microelectron. Nanom. Struct. 11 (1993) 2033–2037. doi:10.1116/1.586539.

[34] V. M. Mikoushkin, V. V. Bryzgalov, E. A. Makarevskaya, A. P. Solonitsyna, D. E. Marchenko, Modification of the GaAs native oxide surface layer into the layer of the Ga2O3 dielectric by an Ar+ ion beam, Surf. Coatings Technol. 344 (2018) 149–153. doi:10.1016/j.surfcoat.2018.03.004.

[35] G. C. Smith, A. K. Livesey, Maximum entropy: A new approach to non- destructive deconvolution of depth profiles from angle- dependent XPS, Surf. Interface Anal. 19 (1992) 175–180. doi:10.1002/sia.740190134.

[36] D. Ensling, R. Hunger, D. Kraft, T. Mayer, W. Jaegermann, M. Rodriguez-Girones, V. Ichizli, H. L. Hartnagel, Pulse plating of Pt on n-GaAs (1 0 0) wafer surfaces: Synchrotron induced photoelectron spectroscopy and XPS of wet fabrication processes, Nucl. Instruments Methods Phys. Res. Sect. B Beam Interact. with Mater. Atoms. 200 (2003) 432–438. doi:10.1016/S0168-583X(02)01735-4.

[37] X.Y. Zhu, T. Huett, M. Wolf, J.M. White, Ultraviolet photochemical nitridation of GaAs Ultraviolet photochemical nitridation of GaAs, Appl. Phys. Lett. 3175 (1992) 127–130. doi:10.1063/1.107950.

[38] S.K. Cheung, N.W. Cheung, Extraction of Schottky diode parameters from forward current-voltage characteristics, Appl. Phys. Lett. 49 (1986) 85–87. doi:10.1063/1.97359.

[39] A.H. Kacha, B. Akkal, Z. Benamara, M. Amrani, A. Rabhi, G. Monier, C. Robert-Goumet, L. Bideux, B. Gruzza, Effects of the GaN layers and the annealing on the electrical properties in the Schottky diodes based on nitrated GaAs, Superlattices Microstruct. 83 (2015) 827–833. doi:10.1016/j.spmi.2015.04.017.

[40] W. P. Leroy, K. Opsomer, S. Forment, R. L. Van Meirhaeghe, The barrier height inhomogeneity in identically prepared Au/n-GaAs Schottky barrier diodes, Solid. State. Electron. 49 (2005) 878–883. doi:10.1016/j.sse.2005.03.005.

[41] M. K. Hudait, S. B. Krupanidhi, Doping dependence of the barrier height and ideality factor of Au/n-GaAs Schottky diodes at low temperatures, Phys. B. 307 (2001) 125–137. doi:10.1016/S0921-4526(01)00631-7.

[42] M. Sağlam, E. Ayyildiz, A. Gümüs, A. Türüt, H. Efeoğlu, S. Tüzemen, Series resistance calculation for the Metal-Insulator-Semiconductor Schottky barrier diodes, Appl. Phys. A. 62 (1996) 269–273. doi:10.1007/s003390050297.

[43] Ş. Karataş, Ş. Altindal, Analysis of I-V characteristics on Au/n-type GaAs Schottky structures in wide temperature range, Mater. Sci. Eng. B. 122 (2005) 133–139. doi:10.1016/j.mseb.2005.05.018.

[44] M. Biber, Ö. Güllü, S. Forment, R. L. Van Meirhaeghe, A. Türüt, The effect of Schottky metal thickness on barrier height inhomogeneity in identically prepared Au/n-GaAs Schottky diodes, Semicond. Sci. Technol. 21 (2006) 1–5. doi:10.1088/0268-1242/21/1/001.

[45] W. E. Spicer, The advanced unified defect model for Schottky barrier formation, J. Vac. Sci. Technol. B. 6 (1988) 1245. doi:10.1116/1.584244.

[46] V. Augelli, T. Ligonzo, A. Minafra, L. Schiavulli, V. Capozzi, G. Perna, M. Ambrico, M. Losurdo, Optical and electrical characterization of n-GaAs surfaces passivated by N2-H2 plasma, J. Lumin. 102–103 (2003) 519–524. doi:10.1016/S0022-2313(02)00603-8.

[47] B. J. Skromme, S. S. Bose, B. Lee, T. S. Low, T. R. Lepkowski, R. Y. DeJule, G. E. Stillman, J. C. M. Hwang, Characterization of high-purity Si-doped molecular beam epitaxial GaAs, J. Appl. Phys. 58 (1985) 4685–4702. doi:10.1063/1.336243.

[48] J. Pastarnak, J. Oswald, M. Laznicka, A. Bosacchi, A. Salokative, The Photoluminescence Spectra of Thin Si-Doped GaAs Layers Grown by MBE, Phys. Stat. Sol. 118 (1990) 567–576.

[49] I. Szafranek, M. A. Plano, M. J. McCollum, S. A. Stockman, S. L. Jackson, K. Y. Cheng, G. E. Stillman, Growth- induced shallow acceptor defect and related luminescence effects in molecular beam epitaxial GaAs, J. Appl. Phys. 68 (1990) 741–754. doi:10.1063/1.346779.

[50] K. Kudo, Y. Makita, I. Takayasu, T. Nomura, T. Kobayashi, T. Izumi, T. Matsumori, Photoluminescence spectra of undoped GaAs grown by molecular-beam epitaxy at very high and low substrate temperatures, J. Appl. Phys. 59 (1986) 888–891. doi:10.1063/1.336559.

[51] V. L. Berkovits, T. V. L 'vova, V. P. Ulin, Chemical nitridation of GaAs(100) by hydrazine sulfide water solutions, Vaccum. 57 (2000) 201–207.

[52] D. M. Tricker, P. D. Brown, T. S. Cheng, C. T. Foxon, C. J. Humphreys, A TEM study of substrate pitting during the MBE growth of GaN on GaAs and GaP substrates, Appl. Surf. Sci. 123–124 (1998) 22–27. doi:10.1016/S0169-4332(97)00475-3.

[53] V.L. Berkovits, D. Paget, a N. Karpenko, V.P. Ulin, O.E. Tereshchenko, Soft nitridation of GaAs(100) by hydrazine sulfide solutions: Effect on surface recombination and surface barrier, Appl. Phys. Lett. 90 (2007) 022104. doi:10.1063/1.2402233.

[54] Y. André, N. Isik Goktas, G. Monier, H. Hijazi, H. Mehdi, C. Bougerol, L. Bideux, A. Trassoudaine, D. Paget, J. Leymarie, E. Gil, C. Robert-Goumet, R.R. LaPierre, Optical and structural analysis of ultra-long GaAs nanowires after nitrogen-plasma passivation, Nano Express. 1 (2020) 020019. doi:10.1088/2632-959X/aba7f1.

[55] H. Hijazi, D. Paget, G. Monier, G. Grégoire, J. Leymarie, E. Gil, F. Cadiz, C. Robert-Goumet, Y. André, Charge and spin transport over record distances in GaAs metallic n-type nanowires: I photocarrier transport in a dense Fermi sea, 2020.